

Tumor suppression by p53 in the absence of Atm

S. Lawrence Bailey², Kay E. Gurley², Kyung Hoon-Kim¹, Karen S. Kelly-Spratt², and Christopher J. Kemp^{2*}

¹Current address: Trubion Pharmaceuticals
Seattle WA 98121

² Fred Hutchinson Cancer Research Center
1100 Fairview Ave N.
Seattle WA, 90109-1024, USA

*To whom correspondence should be addressed:

Tel: 206-667-4252

Fax: 206-667-5815

E-mail: cjkemp@fhcrc.org

Running title: Tumor suppression by Atm and p53

Key words: Squamous cell carcinoma, Trp53, DNA damage, Hras, apoptosis.

Abbreviations: ATM, ataxia telangiectasia mutated; IR, irradiation; dsb, double strand break

Abstract

Oncogenes can induce p53 through a signaling pathway involving p19/Arf. It was recently proposed that oncogenes can also induce DNA damage and this can induce p53 through the Atm DNA damage pathway. To assess the relative roles of Atm, Arf, and p53 in suppression of Ras-driven tumors we examined susceptibility to skin carcinogenesis in DMBA/TPA treated Atm and p53 deficient mice and compared these results to previous studies on Arf deficient mice. Mice with epidermal specific deletion of p53 showed increased papilloma number and progression to malignant invasive carcinomas compared to wild type littermates. In contrast, Atm deficient mice showed no increase in papilloma number, growth, or malignant progression. γ -H2AX and p53 levels were increased in both *Atm*^{+/+} and *Atm*^{-/-} papillomas, while *Arf*^{-/-} papillomas showed much lower p53 expression. Thus although there is evidence of DNA damage, signaling through Arf appears to regulate p53 in these Ras-driven tumors. In spontaneous and radiation induced lymphoma models, tumor latency was accelerated in *Atm*^{-/-}*p53*^{-/-} compound mutant mice compared to the single mutant *Atm*^{-/-} or *p53*^{-/-} mice, indicating cooperation between loss of Atm and loss of p53. Although p53 mediated apoptosis was impaired in irradiated *Atm*^{-/-} lymphocytes, p53 loss was still selected for during lymphomagenesis in *Atm*^{-/-} mice. In conclusion, in these models of oncogene or DNA damage induced tumors, p53 retains tumor suppressor activity in the absence of Atm.

Introduction.

Carcinogenesis is an evolutionary process driven by mutation and selection²⁵. In order to intervene in cancer development, it is important to understand the selective pressures which drive tumor evolution. The observation that p53 mutations are found at high frequency in most types of human cancers¹⁸ indicates selection for cells which have disabled p53 is a nearly universal feature of cancer. p53 can be activated by numerous stressors including DNA damage, oncogene activation, abnormal cell adhesion, altered ribonucleotide pools, hypoxia, telomere erosion, and nutrient deprivation^{15,48}. Activated p53 in turn, can suppress tumor development through the induction of cell cycle arrest, senescence, or apoptosis⁴⁸. Of the many signals that have been reported to phosphorylate and activate p53, it is unclear which of these is physiologically relevant for tumor suppression *in vivo*. This is further complicated by variations between tissues and tumor etiology. DNA damage and activated oncogenes play direct causal roles in cancer induction and p53 activation and so both are reasonable candidates for generating selective pressure against p53 during tumor progression.

DNA damage is the best studied activator of p53. DNA double strand breaks (dsbs), which can be induced by ionizing radiation (IR) or other genotoxic agents, trigger a signaling cascade leading to p53-dependent cell cycle arrest or apoptosis. The protein kinase ATM, which is mutated in the inherited syndrome ataxia telangiectasia (AT), is a primary signal transducer for the cellular response to dsbs⁴³. DNA dsbs activate ATM, which can directly phosphorylate p53 on Ser15^{1;8}. ATM also phosphorylates Chk2, which in turn phosphorylates p53 on Ser 20^{9;42}. ATM impairs the activity of negative regulators of p53, including the ubiquitin ligases cop1 and mdm2^{14;34}. Collectively, these alterations lead to the rapid accumulation of p53 and activation of its

transcriptional functions, which, in turn, can trigger cellular responses such as cell cycle arrest or apoptosis.

AT patients carry homozygous mutations in *ATM* and have an increased risk of developing lymphoreticular malignancies¹¹. *Atm* knockout mice are highly susceptible to lymphoid malignancies, but have not shown a marked predisposition to tumors in other tissues^{3;50}. The basis for this tissue specificity is not known. Westphal *et al.* reported that loss of *Atm* and p53 cooperate to suppress spontaneous development of lymphomas⁴⁹. Liao *et al.* demonstrated that p53 dependent tumor suppression in a mouse brain tumor model driven by truncated SV40 T antigen is unaffected by *Atm* deficiency³¹. In these mouse models, *Atm* does not appear to be an essential regulator of the tumor suppressor function of p53. Several recent studies showed that *Atm* deficiency accelerates *Myc* and mutant *Apc* driven tumors suggesting *Atm* plays role in these tumor models^{29;32;38}.

Atm-dependent signaling *in vivo* is markedly tissue specific. *Atm*^{-/-} mice have impaired p53-dependent apoptosis in irradiated lymphoid tissue and the developing central nervous system as compared to wild type mice^{2;20;51}. However, after a slight delay, p53 induction and apoptotic responses are largely intact in epithelial cells within hair follicles and intestinal crypts from irradiated *Atm* null mice¹⁷. This indicates *Atm* plays a critical role in DNA damage triggered apoptosis in lymphoid cells but there are alternative pathways in epithelial tissues which can compensate in the absence of *Atm*. The presence of redundant DNA damaging signaling pathways in some tissues such as epithelium may explain the narrow tumor spectrum observed in *Atm* deficient mice.

A long standing question concerning the model where DNA damage provides selective pressure against p53 is the source of DNA damage in tumors. Several recent studies showed that

pre-malignant human lesions have constitutively active DNA damage signaling, as determined by staining for γ -H2AX, activated ATM, CHK-2, and p53^{4;16}. It was further shown that oncogenes such as Ras can induce DNA damage and Atm signaling which can then trigger p53-mediated senescence and tumor suppression^{5;12}. Here we test the role of Atm during tumor evolution by comparing the effects of Atm and p53 loss in epithelial and lymphoid tumor models.

Results

We first tested the role of Atm in suppressing Ras-driven tumors by examining the susceptibility of Atm deficient mice to DMBA/TPA induced skin tumors. This protocol involves the topical application of the carcinogen DMBA to the dorsal skin, followed by twice weekly applications of the tumor promoter TPA. This induces benign squamous cell papillomas, a small percentage of which can progress to malignant squamous cell carcinomas after a long latency. Mutation of *Hras* is the initiating event in this tumor model and is detected in ~90% of both papillomas and carcinomas³⁹. Mutational inactivation of p53 occurs late and is strongly associated with papilloma to carcinoma conversion⁷. A causal role for p53 in malignant progression was established using germline *p53* knockout mice, which showed a markedly accelerated rate of carcinoma formation²⁶. That mutations in *Hras* and *p53* occur reproducibly at defined stages in this model facilitates the evaluation of the interaction between Atm with these cancer genes in the context of developing autochthonous tumors.

100% of DMBA/TPA treated *Atm*^{+/+}, *Atm*^{+/-}, and *Atm*^{-/-} mice developed papillomas, which first appeared between 7-9 weeks post-DMBA treatment. The average number of papillomas per mouse was similar for all genotypes through 25 weeks of observation (Figure 1B). The growth rate of papillomas, as measured by tumor size was also similar for all genotypes through 15 weeks, but

slightly reduced in *Atm* null mice after 15 weeks (Figure 1A). Carcinomas first appeared in *Atm*^{+/+}, *Atm*^{+/-}, and *Atm*^{-/-} mice at 15, 22, and 25 weeks, respectively. The latency to carcinoma formation is shown by Kaplan-Meier plots in Figure 1C. The median age for carcinoma development was 29, 32, and 27 weeks for *Atm*^{+/+}, *Atm*^{+/-}, and *Atm*^{-/-} mice, respectively and these values were not significantly different. However during the course of this study, many *Atm* null mice died of lymphomas (Figure 1D), and some of these died before any reasonable chance of progression to carcinomas. Therefore we also analyzed the conversion frequency of papillomas to carcinomas for mice that lived at least 20 weeks post DMBA. Table 1 shows the percentage of papillomas that progressed to carcinomas was 5.6%, 8.3% and 5.0% in *Atm*^{+/+}, *Atm*^{+/-} and *Atm*^{-/-} mice respectively. These frequencies were not significantly different using the two-sided Fisher's exact test. Taken together, these results show that homozygous or hemizygous *Atm* deficiency did not significantly enhance *Hras*-driven tumor number, growth rate, or malignant progression.

In order to compare these results to the effects of p53 loss on skin tumor progression, we repeated the DMBA/TPA protocol on p53 deficient mice. We previously reported accelerated malignant progression in germline p53 deficient mice²⁶ and here we show similar effects with conditional p53 deficient mice (see Materials and Methods)²³. The average number of papillomas was similar between *Trp53*^{F2-10/F2-10}; *K14-Cre* (skin-specific p53 deficient) mice compared to *Trp53*^{F2-10/F2-10} (p53 wild type) mice through 15 weeks. However, new tumors continued to appear in p53 deficient mice after this time, while plateauing in the wild types (Figure 1E). Carcinomas first appeared in *Trp53*^{F2-10/F2-10}; *K14-Cre* mice at 15 weeks and by 30 weeks, 75% of conditional p53 deficient mice averaged 2 carcinomas per mouse (Figure 1F). In contrast, wild type littermates did not develop any carcinomas until after 30 weeks. This difference was highly significant (p=0.001). Thus, skin-specific p53 deletion markedly accelerates malignant skin tumor progression, a result similar to

that seen in p53 germline nullizygous mice^{24;26}. This establishes that the effect of p53 on inhibiting malignant progression is tumor cell autonomous. Both the *Atm* and p53 skin tumor studies were done using littermate wild type controls. This is important as the wild type mice from the two studies differed in carcinoma susceptibility, likely due to different genetic backgrounds (see Materials and Methods). Comparison between these two skin tumor studies reveals that p53 has a more significant impact on suppressing Ras-driven tumor progression than does *Atm*.

We next addressed if DNA damage signaling was prominent in papillomas and if this led to *Atm*-dependent expression of p53. H2AX is rapidly phosphorylated in response to DNA double strand breaks⁴⁰ and phospho-H2AX (γ -H2AX) is widely used as a marker of DNA damage. However γ -H2AX also increases in M phase cells without DNA damage^{21;35} and can be readily detected in epithelial cells during the hair cycle phase in untreated mouse skin²⁸. Staining for γ -H2AX was seen in the occasional cell within the hair follicle of normal skin and in basal and suprabasal cells of the papillomas (Figure 2A). Although *Atm* can phosphorylate H2AX after IR⁴⁴ we observed similar levels of γ -H2AX staining in papillomas from *Atm*^{+/+} and *Atm*^{-/-} mice indicating there are kinases that can substitute for *Atm* to phosphorylate H2AX *in vivo*. Despite γ -H2AX staining, phospho-Chk2, a marker of DNA damage signaling, was low or undetectable in both *Atm*^{+/+} and *Atm*^{-/-} papillomas (Figure 2B). As a positive control, staining for p-Chk2 was seen in irradiated intestinal crypts (data not shown). p53 was undetectable in normal skin but prominent in papillomas and primarily localized to keratinocytes within the basal layer (Figure 2). Equivalent levels and cellular distribution patterns of p53 staining were seen in papillomas from *Atm*^{+/+} and *Atm*^{-/-} mice. Expression of the p53 regulated gene p21 (*Cdkn1a*), and the Cdk inhibitor p16 (*Ink4a*), were also seen in both *Atm*^{+/+} and *Atm*^{-/-} papillomas. As another measure of p53 functionality, we quantified proliferation and apoptosis. The mitotic index was similar in papillomas

from *Atm*^{+/+} and *Atm*^{-/-} mice, while the apoptotic index, as measured by both active caspase 3 and apoptotic figures, was slightly elevated in *Atm*^{-/-} papillomas (Figure 2B). Thus *Atm* deficiency did not measurably affect levels of H2AX, p53, p21, or cell proliferation in benign tumors.

It is useful to compare these results to those seen in p19/Arf null mice. Arf is a tumor suppressor that induces p53 in response to oncogenic activation^{36;41}. We previously showed accelerated papilloma to carcinoma progression in Arf deficient mice using an identical DMBA/TPA protocol²⁴. In comparison to papillomas from wild type and *Atm* null mice, *Arf* null papillomas showed reduced p53 expression and higher H2AX staining and increased mitotic activity (Figure 2). This confirms our previous findings that Arf plays a critical role in the induction of p53 during benign tumor growth. Reduced p53 could explain the increased proliferation in these tumors and this may contribute to increased levels of H2AX. However the DNA damage p53 pathway is still functional in these tumors as irradiated tumor bearing *Arf*^{-/-} mice showed robust p53 induction in papillomas²⁴. These findings, together with the low levels of pChk2 in untreated papillomas, shows that the levels of DNA damage in untreated tumors may be insufficient to trigger a DNA damage response. Thus tumor suppression by p53, at least in this model of epithelial cancer, is regulated by Arf and selection against p53 is driven by oncogenic signaling through Arf.

Compared to epidermal cells, *Atm* has a more critical role in regulating p53 in lymphoid cells¹⁷, so we also examined the interaction of *Atm* and p53 in spontaneous and IR induced lymphoma models. The latency for spontaneous tumor development in *Atm*^{-/-} mice (median age of death=116 days) was shorter than for *p53*^{-/-} mice (median=141 days) (Figure 3A). Tumor latency was significantly accelerated in *Atm*^{-/-} *p53*^{-/-} compound mutant mice (median=84 days) relative to either single mutant alone, consistent with a previous study⁴⁹. ~95% of *Atm*^{-/-} and *Atm*^{-/-} *p53*^{-/-} mice developed CD3 positive T cell lymphomas, which presented as enlarged thymi, with

occasional splenic or lymph node involvement. The tumor spectrum differed slightly in the *p53* nulls. 60% developed thymic lymphoma and 40% developed other tumor types, mainly sarcomas (Table 2). Thus, the reduced tumor latency in *Atm*^{-/-} *p53*^{-/-} mice was mainly due to acceleration of T cell thymic lymphomas.

IR-induced *p53* expression and apoptosis is markedly impaired in thymic lymphoid cells from adult *Atm* null mice⁵¹, indicating *Atm* plays a central role in regulating *p53* and apoptosis in these cells. We first verified that IR-induced apoptosis was impaired in thymocytes from young *Atm* deficient mice. Results shown in Figure 3C show reduced apoptosis in irradiated *Atm*^{-/-} thymus compared to wild type littermates. If this *Atm*-dependent apoptotic pathway is critical for tumor suppression, a prediction is that germline *Atm* deficiency should effectively neutralize *p53* in a radiation-induced tumor model. An additional cohort of mice was treated at two days of age with a single dose of 1.4 Gy. Neonatal radiation reduced latency to tumor development in *p53*^{-/-} mice from a median of 141 days to 100 days (Figure 3B). However, radiation did not noticeably affect tumor development in *Atm*^{-/-} mice. The median age to tumor development in irradiated *Atm*^{-/-} mice was 113 days compared to 116 days in the non-irradiated cohort. Tumor latency in irradiated *Atm*^{-/-} *p53*^{-/-} compound mutants (median = 72 days) was again reduced compared to either single mutant alone. The predominant tumor type in all irradiated genotypes was CD3 positive T cell lymphomas, with a 95% incidence (Table 2).

We next asked if loss of *Atm* reduced or eliminated selection against *p53* during tumor development by examining loss of heterozygosity (LOH) of *p53* in tumors from *Atm*^{-/-} *p53*^{+/-} mice. 50% (4/8) of spontaneous thymic lymphomas and 89% (8/9) of IR-induced lymphomas from *Atm*^{-/-} *p53*^{+/-} mice showed loss of the wild type *p53* allele (Figure 4). This is comparable to 57% (4/7) loss of *p53* in lymphomas from *p53*^{+/-} mice (Figure 4) and the range of 43-75% *p53* LOH reported

in previous studies^{19;22;27;37}. Thus, p53 loss occurs in tumors with or without the presence of Atm. Even under conditions where IR-induced p53-dependent apoptosis is disabled due to loss of Atm, selection against p53 remains. This indicates that although Atm regulates p53 dependent apoptosis in response to acute DNA damage, other Atm independent pathways influence the tumor suppressor function of p53, even in a tumor model where DNA damage was the inducing agent. This also implies that apoptosis is not the only mechanism of tumor suppression by p53.

Discussion

Here, we used three mouse models to compare the roles of Atm and p53 in suppression of oncogene and DNA damage induced tumor development. We first compared the effect of deletion of Atm and p53 on progression of chemically induced skin tumors. ~90% of DMBA/TPA induced papillomas have *Hras* mutations and these tumors showed increased staining for γ -H2AX, p53 and p21 compared to normal skin. However staining for these markers was not significantly reduced in *Atm* null tumors indicating Atm is not required for activation of this tumor suppressor pathway in this autochthonous tumor model. This is consistent with previous results showing that Atm is dispensable for acute IR induced p53 and apoptosis in epidermal hair follicle cells¹⁷. p53 can be activated by DNA damage in an Atm independent manner, for example through Atr, and these other pathways may compensate for the loss of Atm in regulating p53 in this tissue³³.

Compared to wild type and *Atm* null tumors, *Arf* null tumors showed very little p53 expression and increased proliferation. This indicates a central role for *Arf* in regulating p53 during tumor growth. That acute ionizing radiation was able to induce p53 in *Arf* null tumors²⁴, shows that exogenous DNA damage can induce p53 in tumors in the absence of *Arf*. This further implies that the levels of

endogenous DNA damage or damage induced signaling which is present in untreated tumors may be insufficient to activate p53.

The effects of *Atm*, *Arf*, and p53 on tumor progression were consistent with these signaling results. Deletion of both p53 and *Arf* but not *Atm* markedly accelerated the progression of benign papillomas to invasive malignant carcinomas. In wild type mice, p53 loss is strongly selected for during progression of papillomas to carcinomas and p53 loss was less frequent in *Arf* null carcinomas. Together these results show that signaling through *Arf* induces p53 and this provides significant selective pressure against p53.

We also found that the latencies for both spontaneous and radiation-induced lymphomas were accelerated in *Atm* p53 compound mutant mice relative to either single mutant alone. This shows that loss of *Atm* and p53 can cooperate to accelerate tumor formation, and that p53 retains tumor suppressor activity in the absence of *Atm*. Frequent loss of p53 in lymphomas from *Atm*^{-/-} *p53*^{+/-} mice indicates that selection against p53 does not require *Atm*, even in tumors induced by DNA damaging ionizing radiation. This was surprising as IR-induced p53 expression and apoptosis is impaired in *Atm* null lymphocytes. Our results are in general agreement with an elegant study by Christophorou *et al.*, which showed that DNA damage-induced apoptosis is irrelevant for tumor suppression by p53¹⁰. In that study, selection against p53 was instead driven by oncogene-mediated signaling through the p19/*Arf* tumor suppressor. Liao and Van Dyke also concluded that there were two different mechanisms of tumor suppression by *Atm* and p53³⁰. Lymphoma suppression in *Atm* null mice depended on V(D)J recombination, while lymphomas from *p53* null mice arose independently of V(D)J recombination. *Atm* has recently been implicated in repair of V(D)J breaks during antigen receptor rearrangement, and this function could play a role in lymphoma suppression by minimizing oncogenic translocations⁶. Consistent with this idea,

translocations involving the antigen receptors are frequently seen in lymphoid tumors from both AT patients⁴⁵ and *Atm*^{-/-} mice^{2;51}.

In summary, the requirement for *Atm* in regulating p53 in response to DNA damage varies between tissues and this may at least partially explain the tissue specific role of *Atm* in tumor suppression.

In the tumor models we examined, loss of *Atm* did not phenocopy the loss of p53; that is, p53 retained significant tumor suppressor activity in the absence of *Atm*. This highlights that there are multiple and in some cases redundant signals that can activate p53 during tumor suppression. In the case of Ras-driven skin tumors, *Arf* appears to play a more significant role than *Atm* in p53 regulation and tumor progression. Identifying the rate limiting steps in tumor progression in different tumor models and under different tumor etiologies remains an important goal in cancer research. In the broader picture, understanding the nature of the selective pressures that drive tumor evolution is a necessary step to designing effective, mechanistically-based interventions.

Materials and Methods:

Mice. F1 NIH/FVB;129 *Trp53*^{F2-10/+} mice²³ were crossed to N1 NIH/C57 *K14-Cre* mice⁴⁷ and progeny intercrossed to generate experimental mice with the genotypes *Trp53*^{F2-10/F2-10} (p53 WT) and *Trp53*^{F2-10/F2-10}; *K14-Cre* (skin-specific p53 deficient). PCR analysis confirmed that p53 was deleted in epidermis, but not liver, spleen, or thymus. The backs of 8 week old p53 functional WT (n=22), and p53 functional null (n=29) mice were shaved and treated with a single application of DMBA (Sigma; 25 µg in 200 µl acetone) followed a week later by twice weekly applications of TPA (Sigma; 200 µl of 10⁻⁴ M solution in acetone) for 15 weeks. The number and size of papillomas on each mouse was recorded every week. Mice were sacrificed if moribund or one to three weeks following detection of carcinomas. All major organs were examined and tumors were frozen for

DNA extraction and/or fixed in formalin to be processed and stained with H&E for histological examination. For the *Atm* skin tumor study, the *Atm* knockout allele was backcrossed 13 times to the susceptible NIH/Ola strain (Harlan Olac, UK). Experimental mice of all three *Atm* genotypes were then generated from NIH/Ola *Atm*^{+/-} breeders. *Atm*^{-/-} (n=18), *Atm*^{+/-} (n=34), and *Atm*^{+/+} (n=25) mice were treated as above. For the spontaneous and radiation induced tumor models, 129/SvEv *Atm*^{+/-}³ and C57BL6 *p53*^{+/-} mice¹³ were intercrossed to generate experimental mice of the requisite combined *Atm* and *p53* genotypes. One cohort was left untreated and an additional cohort was irradiated at two days of age (1.4 Gy, using a ⁶⁰Co irradiator). Experimental mice were sacrificed and necropsied when exhibiting symptoms of tumor burden.

Histological Analysis. Sections of normal or tumor tissue were removed and either snap frozen or fixed for four hours in normal buffered formalin (NBF) and then processed to paraffin. 4 μm sections were cut, deparaffinized and stained for H&E, p53 (Novocastra CM5), p21 (BD Pharmingen), p16 (Abcam), cleaved caspase-3 (Asp175) (Cell Signaling Tech 9661), phospho-histone H2A.X (Ser139) (Cell Signaling Tech 2577), or phospho-Chk2 (T68) (Abcam). P19/Arf^{-/-} papillomas stained for p53 were from a previous study²⁴. Staining for all antibodies was done using a three step streptavidin technique. Sections were rehydrated and treated with high heat antigen retrieval using a 10mM citrate buffer (pH 6) and then stained with primary Ab. After staining with the primary antibody the sections were stained with a biotin conjugated secondary (Vector labs) followed by StreptABComplex/HRP (DAKO). Slides were developed with DAB/NiCl and counterstained with methyl green. Control sections with no primary antibody were run concurrently. Other sections were cut and stained with H&E. Apoptosis, proliferation and labeling indices were determined by counting the number of stained cells/400x field in five to seven

papillomas per Atm genotype. All counts were done on a Nikon Labophot-2 microscope without knowledge of genotype.

p53 loss of heterozygosity. Genomic DNA was prepared from tumor tissue or normal kidney by QIAamp DNA Mini Kit (QIAGEN). Wild type and knockout alleles of p53 from tumors from *p53+/-* mice were amplified in a separate reaction as described ⁴⁶ for 30 cycles. PCR products were electrophoresed on a 2% TAE agarose gel. Comparison gradients for p53 were established by combining wild type and knockout genomic DNA in quantified ratios, then amplifying as described above.

ReferencesReference List

1. Banin, S., Moyal, L., Shieh, S., Taya, Y., Anderson, C. W., Chessa, L., Smorodinsky, NI, Prives, C., Reiss, Y., Shiloh, Y., and Ziv, Y. Enhanced phosphorylation of p53 by ATM in response to DNA damage. *Science*, 281: 1674-1677, 1998.
2. Barlow, C., Brown, K. D., Deng, C. X., Tagle, D. A., and Wynshaw-Boris, A. Atm selectively regulates distinct p53-dependent cell-cycle checkpoint and apoptotic pathways. *Nature Genet.*, 17: 453-456, 1997.
3. Barlow, C., Hirotsume, S., Paylor, R., Liyanage, M., Eckhaus, M., Collins, F., Shiloh, Y., Crawley, J. N., Ried, T., Tagle, D., and Wynshaw-Boris, A. Atm-deficient mice: a paradigm of ataxia telangiectasia. *Cell*, 86: 159-171, 1996.
4. Bartkova, J., Horejsi, Z., Koed, K., Kramer, A., Tort, F., Zieger, K., Guldborg, P., Sehested, M., Nesland, J. M., Lukas, C., Orntoft, T., Lukas, J., and Bartek, J. DNA damage response

as a candidate anti-cancer barrier in early human tumorigenesis. *Nature*, 434: 864-870, 2005.

5. Bartkova, J., Rezaei, N., Liontos, M., Karakaidos, P., Kletsas, D., Issaeva, N., Vassiliou, L. V., Kolettas, E., Niforou, K., Zoumpourlis, V. C., Takaoka, M., Nakagawa, H., Tort, F., Fugger, K., Johansson, F., Sehested, M., Andersen, C. L., Dyrskjot, L., Orntoft, T., Lukas, J., Kittas, C., Helleday, T., Halazonetis, T. D., Bartek, J., and Gorgoulis, V. G. Oncogene-induced senescence is part of the tumorigenesis barrier imposed by DNA damage checkpoints. *Nature*, 444: 633-637, 2006.
6. Bredemeyer, A. L., Sharma, G. G., Huang, C. Y., Helmink, B. A., Walker, L. M., Khor, K. C., Nuskey, B., Sullivan, K. E., Pandita, T. K., Bassing, C. H., and Sleckman, B. P. ATM stabilizes DNA double-strand-break complexes during V(D)J recombination. *Nature*, 442: 466-470, 2006.
7. Burns, P. A., Kemp, C. J., Gannon, J. V., Lane, D. P., Bremner, R., and Balmain, A. Loss of heterozygosity and mutational alterations of the p53 gene in skin tumors of interspecific hybrid mice. *Oncogene*, 6: 2363-2369, 1991.
8. Canman, C. E., Lim, D. S., Cimprich, K. A., Taya, Y., Tamai, K., Sakaguchi, K., Appella, E., Kastan, M. B., and Siliciano, J. D. Activation of the ATM kinase by ionizing radiation and phosphorylation of p53. *Science*, 281: 1677-1679, 1998.
9. Chehab, N. H., Malikzay, A., Appel, M., and Halazonetis, T. D. Chk2/hCds1 functions as a DNA damage checkpoint in G(1) by stabilizing p53. *Genes & Dev.*, 14: 278-288, 2000.

10. Christophorou, M. A., Ringshausen, I., Finch, A. J., Swigart, L. B., and Evan, G. I. The pathological response to DNA damage does not contribute to p53-mediated tumour suppression. *Nature*, *443*: 214-217, 2006.
11. Chun, H. H. and Gatti, R. A. Ataxia-telangiectasia, an evolving phenotype. *DNA Repair (Amst)*, *3*: 1187-1196, 2004.
12. Di, M. R., Fumagalli, M., Cicalese, A., Piccinin, S., Gasparini, P., Luise, C., Schurra, C., Garre', M., Nuciforo, P. G., Bensimon, A., Maestro, R., Pelicci, P. G., and d'Adda di Fagagna F. Oncogene-induced senescence is a DNA damage response triggered by DNA hyper-replication. *Nature*, *444*: 638-642, 2006.
13. Donehower, L. A., Harvey, M., Slagle, B. L., McArthur, M. J., Montgomery, C. A., Jr., Butel, J. S., and Bradley, A. Mice deficient for p53 are developmentally normal but susceptible to spontaneous tumours. *Nature*, *356*: 215-221, 1992.
14. Dornan, D., Shimizu, H., Mah, A., Dudhela, T., Eby, M., O'rourke, K., Seshagiri, S., and Dixit, V. M. ATM engages autodegradation of the E3 ubiquitin ligase COP1 after DNA damage. *Science*, *313*: 1122-1126, 2006.
15. Giaccia, A. J. and Kastan, M. B. The complexity of p53 modulation: emerging patterns from divergent signals. *Genes & Dev.*, *12*: 2973-2983, 1998.
16. Gorgoulis, V. G., Vassiliou, L. V., Karakaidos, P., Zacharatos, P., Kotsinas, A., Liloglou, T., Venere, M., DiTullio, R. A., Jr., Kastriakis, N. G., Levy, B., Kletsas, D., Yoneta, A., Herlyn, M., Kittas, C., and Halazonetis, T. D. Activation of the DNA damage checkpoint and genomic instability in human precancerous lesions. *Nature*, *434*: 907-913, 2005.

17. Gurley, K. E. and Kemp, C. J. Atm is not required for p53 induction and apoptosis in irradiated epithelial tissues. *Mol. Cancer Res.*, 5: 1312-1318, 2007.
18. Hainaut, P. and Hollstein, M. p53 and human cancer: the first ten thousand mutations. *Adv. Cancer Res.*, 77: 81-137, 2000.
19. Harvey, M., McArthur, M. J., Montgomery, C. A., Jr., Butel, J. S., Bradley, A., and Donehower, L. A. Spontaneous and carcinogen-induced tumorigenesis in p53- deficient mice. *Nature Genet.*, 5: 225-229, 1993.
20. Herzog, K. H., Chong, M. J., Kapsetaki, M., Morgan, J. I., and McKinnon, P. J. Requirement for Atm in ionizing radiation-induced cell death in the developing central nervous system. *Science*, 280: 1089-1091, 1998.
21. Ichijima, Y., Sakasai, R., Okita, N., Asahina, K., Mizutani, S., and Teraoka, H. Phosphorylation of histone H2AX at M phase in human cells without DNA damage response. *Biochem. Biophys. Res. Commun.*, 336: 807-812, 2005.
22. Jacks, T., Remington, L., Williams, B. O., Schmitt, E. M., Halachmi, S., BronsonRT., and Weinberg, R. A. Tumor spectrum analysis in p53-mutant mice. *Curr. Biol.*, 4: 1-7, 1994.
23. Jonkers, J., Meuwissen, R., van der, G. H., Peterse, H., van, d., V, and Berns, A. Synergistic tumor suppressor activity of BRCA2 and p53 in a conditional mouse model for breast cancer. *Nature Genet.*, 29: 418-425, 2001.

24. Kelly-Spratt, K. S., Gurley, K. E., Yasui, Y., and Kemp, C. J. p19Arf suppresses growth, progression, and metastasis of Hras-driven carcinomas through p53-dependent and -independent pathways. *PLoS Biology*, 2: E242, 2004.
25. Kemp, C. J. Multistep skin cancer in mice as a model to study the evolvability of cancer cells. *Sem. Cancer Biol.*, 15: 460-473, 2005.
26. Kemp, C. J., Donehower, L. A., Bradley, A., and Balmain, A. Reduction of p53 gene dosage does not increase initiation or promotion but enhances malignant progression of chemically induced skin tumors. *Cell*, 74: 813-822, 1993.
27. Kemp, C. J., Wheldon, T., and Balmain, A. p53 deficient mice are extremely susceptible to radiation-induced tumorigenesis. *Nature Genet.*, 8: 66-69, 1994.
28. Koike, M., Mashino, M., Sugasawa, J., and Koike, A. Dynamic change of histone H2AX phosphorylation independent of ATM and DNA-PK in mouse skin in situ. *Biochem. Biophys. Res. Commun.*, 363: 1009-1012, 2007.
29. Kwong, L. N., Weiss, K. R., Haigis, K. M., and Dove, W. F. Atm is a negative regulator of intestinal neoplasia. *Oncogene*, 2007.
30. Liao, M. J. and Van Dyke, T. Critical role for Atm in suppressing V(D)J recombination-driven thymic lymphoma. *Genes & Dev.*, 13: 1246-1250, 1999.
31. Liao, M. J., Yin, C., Barlow, C., Wynshaw-Boris, A., and Van Dyke T. Atm is dispensable for p53 apoptosis and tumor suppression triggered by cell cycle dysfunction. *Mol. Cell Biol*, 19: 3095-3102, 1999.

32. Maclean, K. H., Kastan, M. B., and Cleveland, J. L. Atm deficiency affects both apoptosis and proliferation to augment Myc-induced lymphomagenesis
2. *Mol. Cancer Res.*, 5: 705-711, 2007.
33. Matsuoka, S., Ballif, B. A., Smogorzewska, A., McDonald, E. R., III, Hurov, K. E., Luo, J., Bakalarski, C. E., Zhao, Z., Solimini, N., Lerenthal, Y., Shiloh, Y., Gygi, S. P., and Elledge, S. J. ATM and ATR substrate analysis reveals extensive protein networks responsive to DNA damage. *Science*, 316: 1160-1166, 2007.
34. Maya, R., Balass, M., Kim, S. T., Shkedy, D., Leal, J. F., Shifman, O., Moas, M., Buschmann, T., Ronai, Z., Shiloh, Y., Kastan, M. B., Katzir, E., and Oren, M. ATM-dependent phosphorylation of Mdm2 on serine 395: role in p53 activation by DNA damage. *Genes Dev*, 15: 1067-1077, 2001.
35. McManus, K. J. and Hendzel, M. J. ATM-dependent DNA damage-independent mitotic phosphorylation of H2AX in normally growing mammalian cells. *Mol. Biol. Cell*, 16: 5013-5025, 2005.
36. Palmero, I., Pantoja, C., and Serrano, M. p19ARF links the tumour suppressor p53 to Ras. *Nature*, 395: 125-126, 1998.
37. Purdie, C. A., Harrison, D. J., Peter, A., Dobbie, L., White, S., Howie, S. E. M., Salter, D. M., Bird, C. C., Wyllie, A. H., Hooper, M. L., and Clarke, A. R. Tumour incidence, spectrum and ploidy in mice with a large deletion in the p53 gene. *Oncogene*, 9: 603-609, 1994.

38. Pusapati, R. V., Rounbehler, R. J., Hong, S., Powers, J. T., Yan, M., Kiguchi, K., McArthur, M. J., Wong, P. K., and Johnson, D. G. ATM promotes apoptosis and suppresses tumorigenesis in response to Myc. *Proc Natl. Acad. Sci. U. S. A.*, *103*: 1446-1451, 2006.
39. Quintanilla, M., Brown, K., Ramsden, M., and Balmain, A. Carcinogen-specific mutation and amplification of Ha-ras during mouse skin carcinogenesis. *Nature*, *322*: 78-80, 1986.
40. Rogakou, E. P., Pilch, D. R., Orr, A. H., Ivanova, V. S., and Bonner, W. M. DNA double-stranded breaks induce histone H2AX phosphorylation on serine 139. *Journal of Biological Chemistry*, *273*: 5858-5868, 1998.
41. Sherr, C. J. Divorcing ARF and p53: an unsettled case. *Nat Rev Cancer*, *6*: 663-673, 2006.
42. Shieh, S. Y., Ahn, J., Tamai, K., Taya, Y., and Prives, C. The human homologs of checkpoint kinases Chk1 and Cds1 (Chk2) phosphorylate p53 at multiple DNA damage-inducible sites. *Genes Dev*, *14*: 289-300, 2000.
43. Shiloh, Y. The ATM-mediated DNA-damage response: taking shape. *Trends Biochem. Sci.*, *31*: 402-410, 2006.
44. Stiff, T., O'Driscoll, M., Rief, N., Iwabuchi, K., Lobrich, M., and Jeggo, P. A. ATM and DNA-PK function redundantly to phosphorylate H2AX after exposure to ionizing radiation. *Cancer Res.*, *64*: 2390-2396, 2004.
45. Taylor, A. M. R., Metcalfe, J. A., Thick, J., and Mak, Y. F. Leukemia and lymphoma in ataxia telangiectasia. *Blood*, *87*: 423-438, 1996.

46. Timme, T. L. and Thompson, T. C. Rapid allelotype analysis of p53 knockout mice. *Biotechniques*, 17: 462-463, 1994.
47. Vasioukhin, V., Degenstein, L., Wise, B., and Fuchs, E. The magical touch: genome targeting in epidermal stem cells induced by tamoxifen application to mouse skin. *Proc. Natl. Acad. Sci. U. S. A.*, 96: 8551-8556, 1999.
48. Vousden, K. H. and Lu, X. Live or let die: the cell's response to p53. *Nature Rev. Cancer*, 2: 594-604, 2002.
49. Westphal, C. H., Rowan, S., Schmaltz, C., Elson, A., Fisher, D. E., and Leder, P. *atm* and p53 cooperate in apoptosis and suppression of tumorigenesis, but not in resistance to acute radiation toxicity. *Nature Genet.*, 16: 397-401, 1997.
50. Xu, Y., Ashley, T., Brainerd, E. E., Bronson, R. T., Meyn, M. S., and Baltimore, D. Targeted disruption of ATM leads to growth retardation, chromosomal fragmentation during meiosis, immune defects, and thymic lymphoma. *Genes & Dev.*, 10: 2411-2422, 1996.
51. Xu, Y. and Baltimore, D. Dual roles of ATM in the cellular response to radiation and in cell growth control. *Genes & Dev.*, 10: 2401-2410, 1996.

Acknowledgements. We thank Tony Wynshaw-Boris for providing *Atm* null mice and members of the Kemp laboratory for helpful discussions. This work was funded by NIH research grant R01 CA70414 and NIEHS research grant U01 ES11045.

Table 1. Conversion frequency of carcinomas to papillomas for mice that lived at least 20 weeks post DMBA.

Genotype	Number of Mice	Total # of papillomas	Total # of carcinomas	Conversion Frequency	p value vs. <i>ATM</i> +/+
<i>ATM</i> -/-	7	121	6	5.0%	1
<i>ATM</i> +/-	33	664	55	8.3%	0.11
<i>ATM</i> +/+	25	503	28	5.6%	N / A

Table 2. Tumor spectrum in *Atm* (AT) and p53 deficient mice.

	Spontaneous				Irradiated			
	<i>AT</i> -/- <i>p53</i> -/-	<i>AT</i> -/- <i>p53</i> +/-	<i>AT</i> -/- <i>p53</i> +/+	<i>AT</i> +/+ <i>p53</i> -/-	<i>AT</i> -/- <i>p53</i> -/-	<i>AT</i> -/- <i>p53</i> +/-	<i>AT</i> -/- <i>p53</i> +/+	<i>AT</i> +/+ <i>p53</i> -/-
Thymoma/Lymphoma	9	9	12	9	4	11	4	8
Sarcoma	1	0	0	2	0	0	0	1
Testicular Tumor	0	0	0	2	0	0	0	2
Brain Tumor	0	0	0	1	0	0	0	0
Multiple	2	1	0	2	0	0	0	0
Other	1	1	2	1	0	0	1	0
Total	13	11	14	17	4	11	5	11

Figure legends

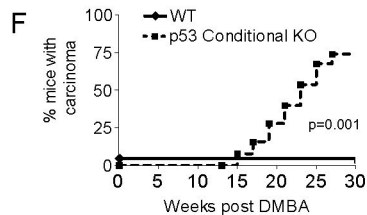
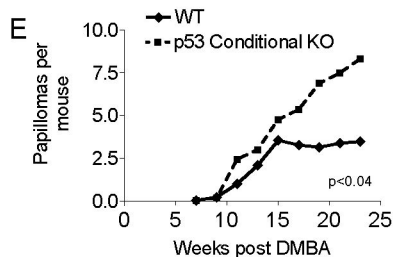
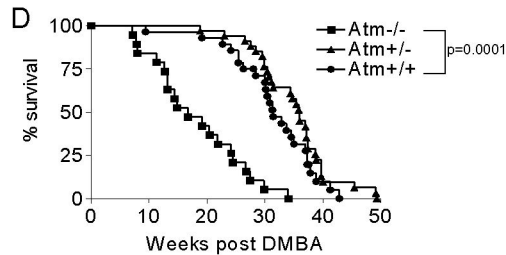
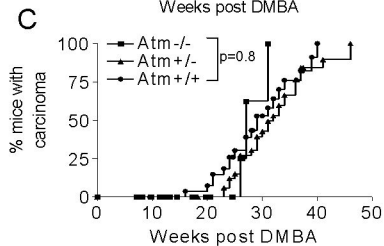
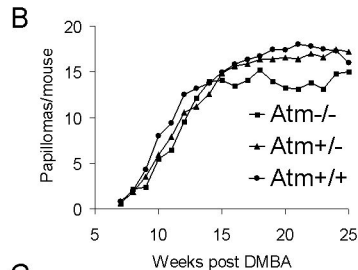
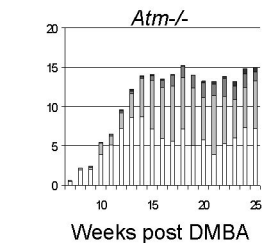
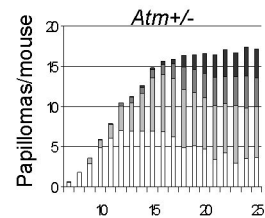
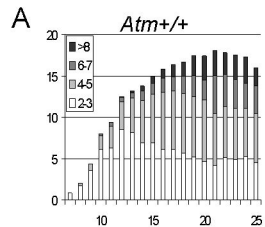
Figure 1: Skin tumor development in *Atm* and p53 deficient mice. **A**, DMBA/TPA induced papillomas in *Atm* deficient mice. The mean number of papillomas per mouse of the indicated size class is plotted over time post DMBA treatment. **B**, The average number of papillomas of all size classes from mice of the indicated *Atm* genotype is plotted over time post DMBA treatment. **C**, Carcinoma free survival in DMBA/TPA treated mice. ($p=0.8$ *Atm*^{-/-} vs *Atm*^{+/+} and $p=0.2$ for *Atm*^{+/-} vs *Atm*^{+/+}, log rank test). **D**, Tumor free survival in DMBA/TPA treated mice. ($p<0.0001$ for *Atm*^{-/-} vs. *Atm*^{+/+} and $p=0.11$ for *Atm*^{+/-} vs. *Atm*^{+/+}, using log rank test). **E**, DMBA/TPA induced papillomas in *Trp53*^{F2-10/F2-10} (p53 WT) and *Trp53*^{F2-10/F2-10}; *K14-Cre* (skin-specific p53 deficient) mice. The number of papillomas in p53 deficient mice at 23 and 25 weeks was greater than wild types ($p=0.003$ and 0.04 respectively, using an unpaired t-test). **F**, Carcinoma free survival in DMBA/TPA treated p53 WT and skin specific p53 deleted mice (p53 conditional KO). The difference was highly significant ($p=0.001$ using the log rank test).

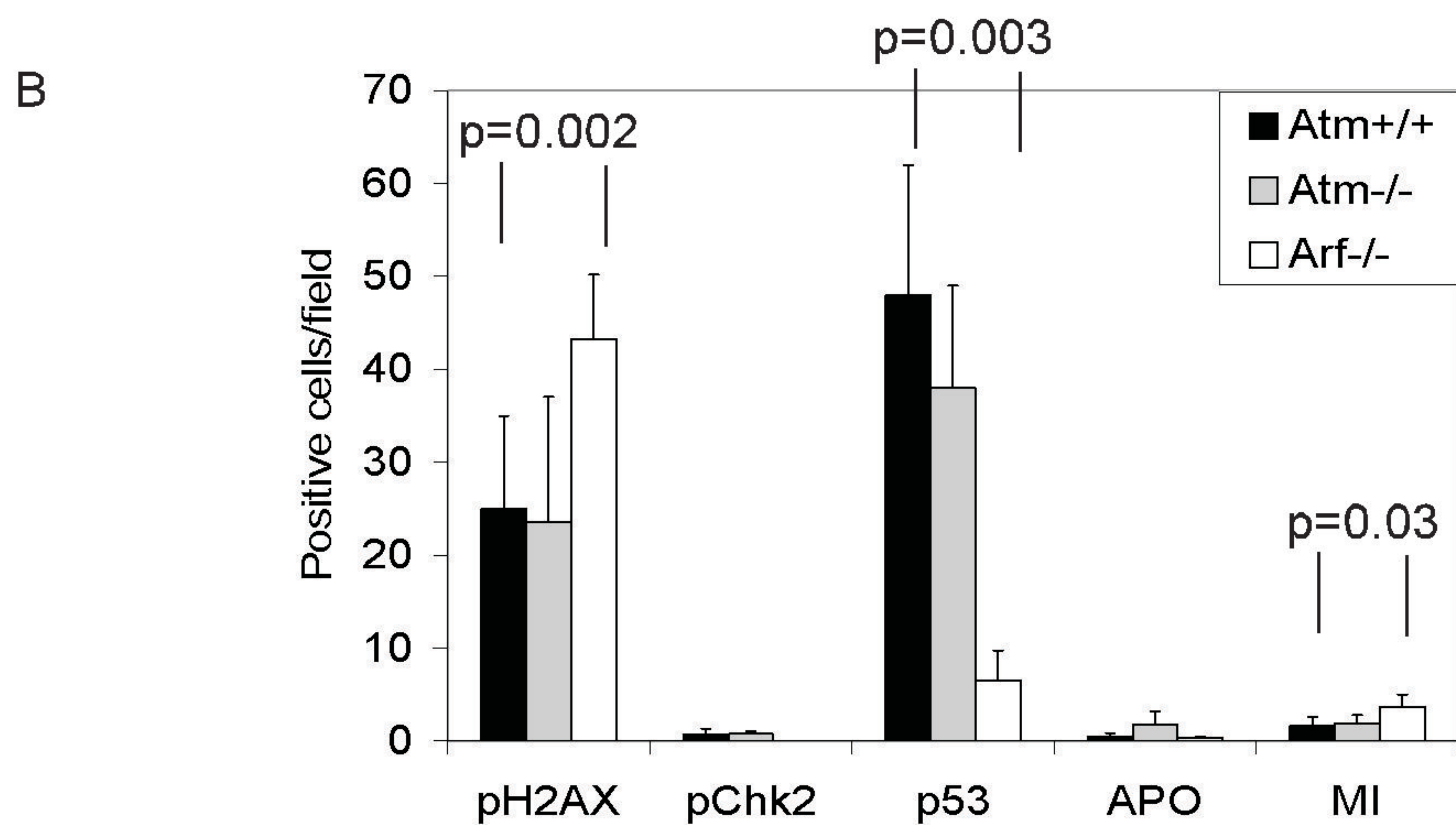
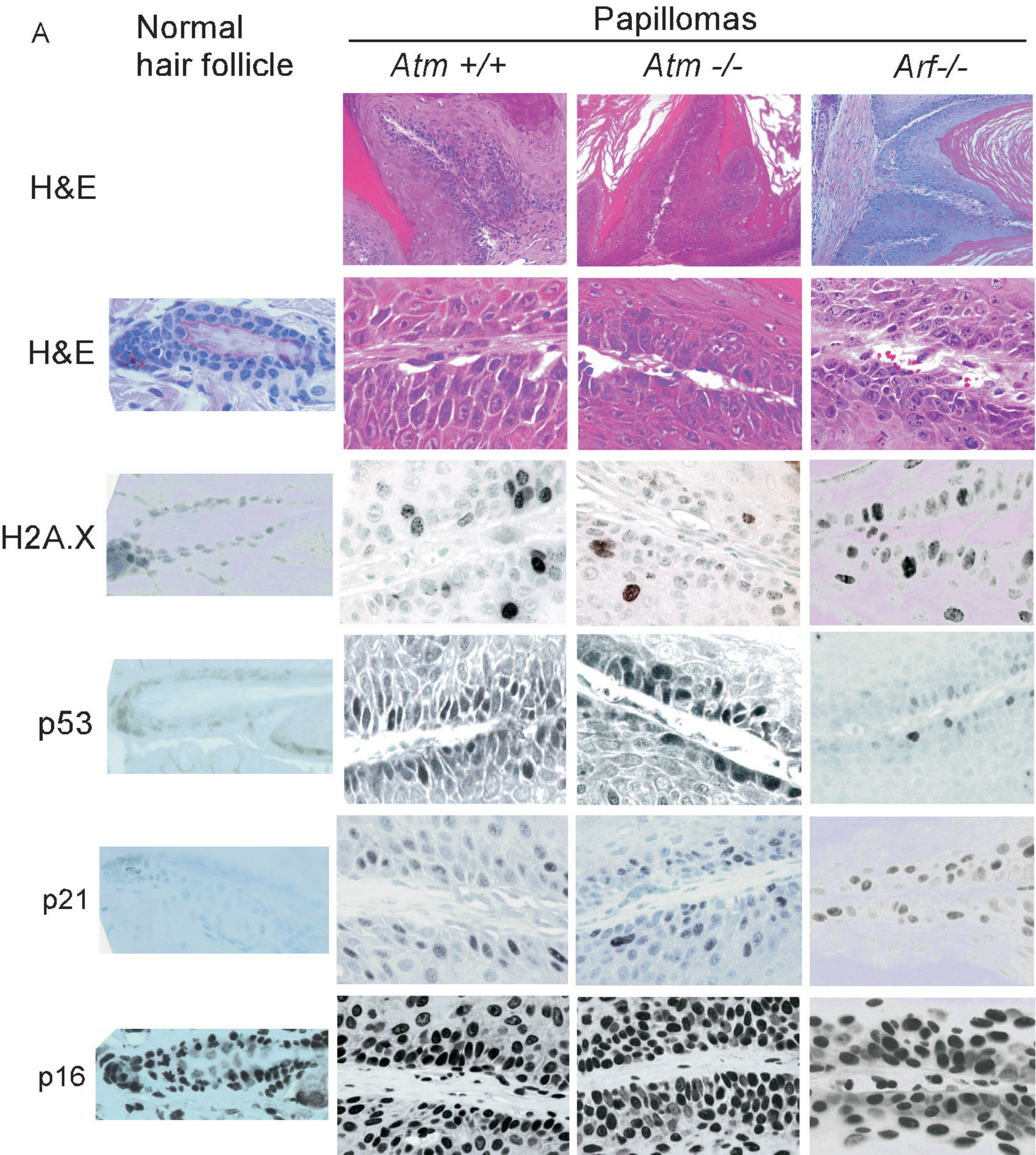
Figure 2: DNA damage signaling in *Atm* deficient papillomas. **A**, H&E stained sections and immunostaining for the indicated proteins from papillomas from wild type, *Atm*^{-/-} and *Arf*^{-/-} mice. Top row was photographed with a final magnification of 100x and lower rows at 600x. **B**, Quantification of γ -H2AX, pChk2, p53, apoptosis, (APO) and mitotic index (MI), in *Atm*^{+/+}, *Atm*^{-/-} and *Arf*^{-/-} papillomas ($n=5-7$ tumors per genotype). The values were calculated as mean plus standard deviation of the number of cells that stained for γ -H2AX, pChk2, p53, or apoptotic or mitotic figures per 400x field. The p values were determined by the Mann-Whitney test.

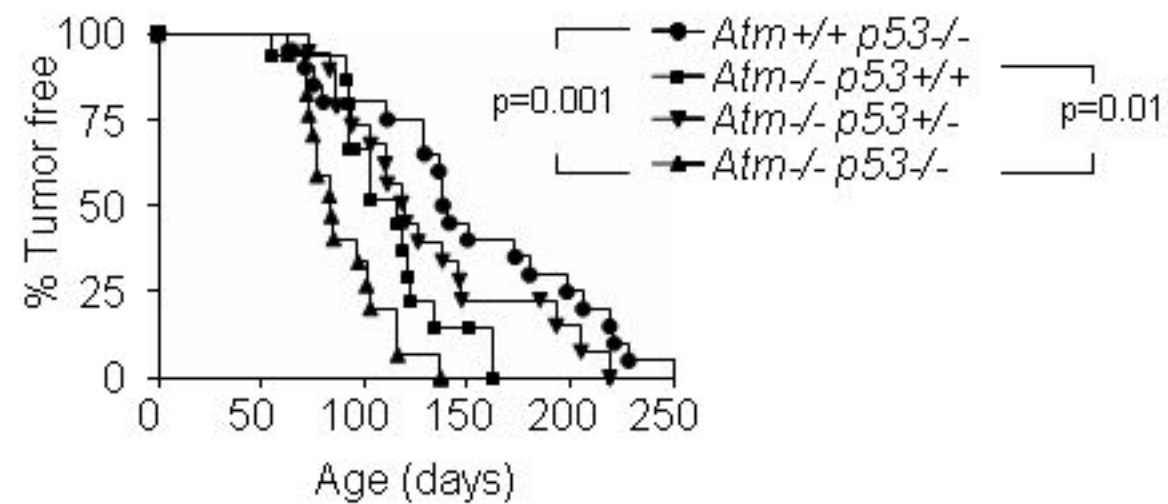
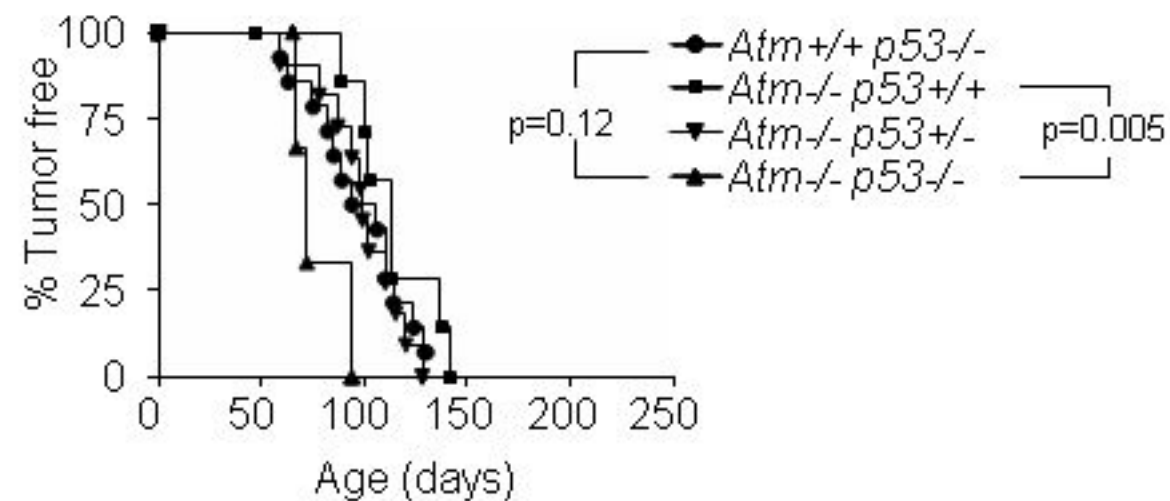
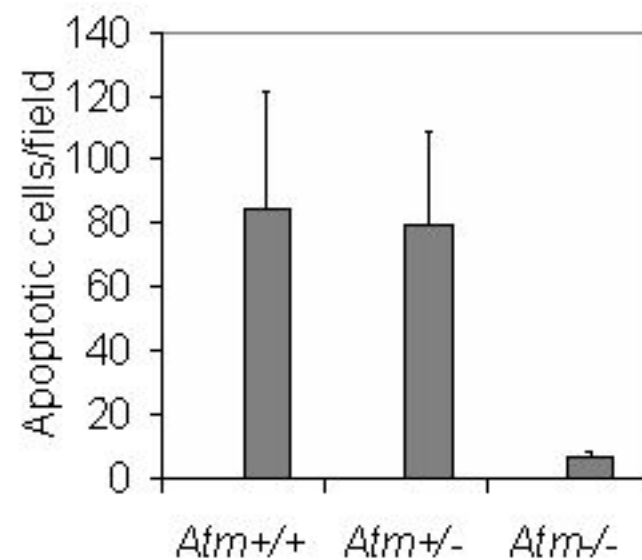
Figure 3: Loss of p53 and *Atm* cooperate during tumorigenesis. **A**, Spontaneous tumor development is accelerated in *Atm*^{-/-}*p53*^{-/-} ($n=13$) mice relative to *Atm*^{-/-} ($n=14$) or *p53*^{-/-} ($n=18$) mice. **B**, IR-induced tumor development is accelerated in all genotypes except *Atm*^{-/-} mice. *Atm*^{-/-}

p53^{-/-} mice (n=4) develop tumors faster than *Atm*^{-/-} (n=8) or *p53*^{-/-} (n=15) mice. **C**, IR induced apoptosis in thymus from 3 week old mice (4 Gy 4 h). The values are mean plus standard deviation of apoptotic figures per 400x field for 3-5 mice per genotype.

Figure 4: p53 LOH is seen in tumors from both *Atm*^{+/+} and *Atm*^{-/-} mice. PCR analysis shows loss of the wild type allele of *p53* in 4/7 spontaneous and 8/9 IR -induced tumors from *Atm*^{-/-}*p53*^{+/-} mice and from 4/7 tumors from *p53*^{+/-} mice. * indicates LOH of *p53* in tumors. wt=wild type *p53* allele, mu= mutant *p53* allele.





A**B****C**

tumor

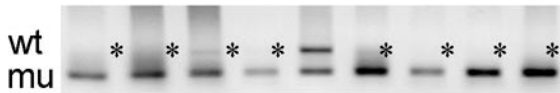
normal

+/+ +/- -/-

Atm^{-/-}p53^{+/-}
spontaneous



Atm^{-/-}p53^{+/-}
irradiated



Atm^{+/+}p53^{+/-}
irradiated

